Two-Dimensional ^{1}H NMR Studies of Cytochrome *c*: Hydrogen Exchange in the N-Terminal Helix†

A. Joshua Wand,‡ Heinrich Roder, and S. Walter Englander*
Department of Biochemistry and Biophysics, University of Pennsylvania, Philadelphia, Pennsylvania 19104
Received June 11, 1985

ABSTRACT: The hydrogen exchange behavior of the N-terminal helical segment in horse heart cytochrome *c* was studied in both the reduced and the oxidized forms by use of two-dimensional nuclear magnetic resonance methods. The amide protons of the first six residues are not H bonded and exchange rapidly with solvent protons. The most N-terminal H-bonded groups—the amide NH of Lys-7 to Phe-10—exhibit a sharp gradient in exchange rate indicative of dynamic fraying behavior, consistent with statistical-mechanical principles. This occurs identically in both reduced and oxidized cytochrome *c*. In the oxidized form, residues 11–14, which form the last helical turn, all exchange with a similar rate, about one million times slower than the rate characteristic of freely exposed peptide NH, even though some are on the aqueous face of the helix and others are fully buried. These and similar observations in several other proteins appear to document local cooperative unfolding reactions as determinants of protein H exchange reactions. The N-terminal segment of cytochrome *c* is insensitive to the heme redox state, as in the crystallographic model, except for residues closest to the heme (Cys-14 and Ala-15), which exchange about 15-fold more slowly in the reduced form. The cytochrome *c* H exchange results can be further considered in terms of the conformation of the native and the transiently unfolded forms and their free energy relationships in both the reduced and the oxidized states.

We are using cytochrome *c* to address the issue of hydrogen exchange mechanism and to learn what hydrogen exchange measurements can reveal concerning a well-defined functional change, the cytochrome *c* redox transition. Hydrogen exchange reactions can provide local probe points all through a protein for monitoring structure, structural dynamics, and the effects on these of functional state (Englander & Kallenbach, 1984). Though a great deal is known about the physical and biological properties of the *c*-type cytochromes [reviewed by Salemme (1977), Dickerson & Timovich (1975), Ferguson-Miller et al. (1979), Moore et al. (1982) and Margoliash & Boshard (1983)], basic questions concerning its molecular function remain unanswered. How does the protein modulate the properties of the heme group to achieve precise adjustment of its redox potential? Various possibilities have been discussed (Kassner, 1972; Stellwagen, 1978; Senn et al., 1980; Moore, 1983; Churg et al., 1983). What is the mechanism and physical basis of electron transfer (Marcus, 1964; Hopfield, 1974; DeVault, 1980; Margoliash & Boshard, 1983)? What is the nature and functional importance of structural changes that couple with the redox transition? Comparison of reduced and oxidized tuna cytochrome *c* by X-ray diffraction has revealed only quite subtle structural changes (Takano & Dickerson, 1981a,b), though other physicochemical studies on denaturation (Margoliash & Schejter, 1966), hydrogen exchange (Ulmer & Kägi, 1965; Patel & Canuel, 1976), and compressibility (Eden et al., 1982) indicate that the reduced form is substantially more stable and rigid.

Our plan is to approach these issues by studying the hydrogen exchange behavior of cytochrome *c* at the ultimate proton-resolved level. This has been attempted before in other proteins, initially by 1D NMR[1] observation of a limited number of amide protons and more recently by 2D NMR observation of essentially all the amide protons in some small proteins (Wagner & Wüthrich, 1982a; Wüthrich et al., 1984). In principle, one can hope to resolve all or most of the protons in cytochrome *c* and to measure their exchange with solvent protons by use of recently emerging two-dimensional NMR techniques (Aue et al., 1976; Freeman & Morris, 1979; Bax, 1982; Wüthrich et al., 1982; Wider et al., 1984). In practice, the size of cytochrome *c* (104 residues in the horse protein) and the relative complexity of its spin systems (e.g., 19 lysines) make the initial problem of assigning its protons in the NMR spectrum a formidable task. So far, this has been accomplished only for proteins just over half this size [e.g., Wagner & Wüthrich (1982b); see also references cited in the preceding paper (Wand & Englander, 1986)].

The exchange studies reported here focus on the N-terminal segment of horse cytochrome *c*. The detailed ^{1}H resonance assignment of this region is documented in the preceding paper (Wand & Englander, 1986). The H exchange results exhibit some of the cooperative H bond breaking motions that underly hydrogen exchange reactions and begin to show parts of the protein that are sensitive to change in redox state.

Experimental Procedures

Materials. Horse heart cytochrome *c* from Sigma Chemical Co. in the highest available grade (type VI) was used without further purification. Sodium ascorbate (Sigma) and potassium ferricyanide (Fisher Scientific) were reagent-grade. For D_2O solutions, pH* is quoted as the pH meter reading measured at room temperature.

† This work was supported by NIH Grants AM 11295 and GM 31847. A.J.W. gratefully acknowledges a Natural Sciences and Engineering Research Council of Canada postgraduate scholarship.
‡ Present address: Institute for Cancer Research, Fox Chase Cancer Center, Philadelphia, PA 19111.

[1] Abbreviations: NMR, nuclear magnetic resonance; COSY, *J*-correlated spectroscopy; NOE, nuclear Overhauser effect; ppm, parts per million; BUSI IIA, proteinase inhibitor IIA from bull seminal plasma.

0006-2960/86/0425-1107$01.50/0

Table I: Hydrogen Exchange in the N-Terminal Cytochrome *c* Segment[a]

	reduced			oxidized		
residue	k_{ex} (h^{-1})	% error	k_c/k_{ex}[b]	k_{ex} (h^{-1})	% error	k_c/k_{ex}[b]
Lys-5	>10		$<4 \times 10^3$	>10		$<4 \times 10^3$
Gly-6	>10		$<4 \times 10^3$	>10		$<4 \times 10^3$
Lys-7	>10		$<4 \times 10^3$	>10		$<4 \times 10^3$
Lys-8	0.63	2	5.1×10^4	1.5	2	2.9×10^4
Ile-9	5×10^{-4}	50	3×10^7	8×10^{-4}	50	3×10^7
Phe-10[c]	10^{-5}–10^{-4}		10^8–10^9	10^{-5}–10^{-4}		10^8–10^9
Val-11	0.016	7	1.0×10^6	0.02	10	1.1×10^6
Gln-12	0.075	14	2.4×10^5	0.12	7	2.1×10^5
Lys-13	0.055	4	4.3×10^5	0.049	4	6.4×10^5
Cys-14	0.0038	7	2.2×10^7	0.083	7	1.3×10^6
Ala-15	0.038	6	6.9×10^5	0.44	11	8.0×10^4

[a] Hydrogen–deuterium exchange rates, k_{ex}, and slowing factors, k_c/k_{ex}, for the amide protons of residues 5–15 in reduced and oxidized horse cytochrome *c* at pH* 7, 20 °C. Exchange rates and relative errors were obtained by exponential least-squares analysis (Figure 4). [b] Intrinsic exchange rates, k_c, were calculated according to Molday et al. (1972) at pH* 6.87 and 6.98 for reduced and oxidized cytochrome *c*, respectively. [c] Estimate of upper rate limit for Phe-10 on the basis of the data in Figure 4; lower limit from extrapolation of data at higher temperature (Patel & Canuel, 1976) to 20 °C.

Hydrogen Exchange. ^1H–^2H exchange was carried out at 20 °C in D_2O and 50 mM phosphate buffer, pH* 7.0. Exchange was initiated by passing 5 mL of an 8 mM ferricytochrome *c* solution in H_2O, previously fully oxidized by addition of 5 mM ferricyanide, over a Sephadex G-25 column (2.5 × 30 cm) equilibrated with D_2O buffer. The eluted cytochrome *c* solution (ca. 4 mM) was separated into two equal volumes. One sample was reduced by addition of a concentrated sodium ascorbate solution in D_2O buffer (pH* 7.0) to a final concentration of 15 mM. To prevent bacterial growth during subsequent long-term H exchange incubations, the solutions were passed through sterile filters (Millipore Miller-GV, 0.22 m). These procedures were carried out at 6 °C and required about 10 min. The final pH* of the oxidized and reduced samples was 6.98 and 6.87, respectively (this small difference was taken into account in the calculation of exchange slowing factors). Both preparations were then incubated at 20 °C to promote ^1H–^2H exchange. The reduced batch was kept under nitrogen. Eight samples were withdrawn from each preparation at logarithmically spaced time points (factors of 3 in time), from 20 min to 1 month. To prepare for the NMR exchange assay, oxidized samples were reduced with ascorbate (as above); then, all samples were adjusted to pH* 5 with dilute HCl and concentrated to 0.4 mL by centrifugal ultrafiltration, resulting in a protein concentration of about 8 mM. The samples were handled at ca. 6 °C and stored frozen at −20 °C pending NMR analysis.

NMR Spectroscopy. Two-dimensional ^1H NMR spectra were recorded at 500 MHz on a Bruker WM 500 spectrometer (Yale University). All measurements were performed with the reduced protein at 20 °C and pH* 5. Two-dimensional *J*-correlated COSY spectra (Aue et al., 1976; Nagayama et al., 1980) were acquired with the pulse sequence

$$(t_0\text{–}90°\text{–}t_1\text{–}90°\text{–}t_2\text{–})_n$$

where t_0 is the relaxation delay, t_1 is the incremented evolution period, and t_2 is the detection period. During t_2, 1024 complex data points were recorded, and 48 scans (plus four dummy scans) were collected for 400 increments of t_1 between 0.124 and 63 ms. Average recycling period was 0.96 s, and total acquisition time was about 6 h. The residual HDO signal was suppressed by weak irradiation at all times except during data acquisition. The carrier frequency was placed in the center of the spectrum, and phase cycling appropriate for quadrature detection in both dimensions was used. Prior to Fourier transformation, the data were multiplied in both dimensions by an unshifted sine bell filter function, and the t_1 domain data were zero-filled to 1024 points. An absolute magnitude calculation was performed. Final digital resolution was 7.9 Hz/point.

The intensity, *I*, of NH–C_αH cross peaks was determined by calculating the cross-peak volume integral, covering a radius of six to seven data points for well-isolated cross peaks and a smaller radius for partially overlapped peaks. An average of 20 volume readings in empty regions of the spectrum was used as a background value, *b*. Where a cross peak was partially overlapped with a more slowly exchanging peak, additional background subtraction was necessary. For each spectrum, the average volume of four cross peaks between nonexchangeable protons was used as an internal intensity reference, I_{ref}. For this, the C_5H–C_6H and C_6H–C_7H cross peaks of Trp-59 and the bridge 2 and bridge 4 methine–methyl cross peaks were used. Exchange rates were then determined by exponential regression of $(I-b)/(I_{ref}-b)$ vs. exchange time. Processing and manipulation of the NMR data were done on a VAX 11/750 using a program kindly provided by D. Hare.

Results

Two-dimensional *J*-correlated (COSY) spectroscopy was used to monitor the ^1H–^2H exchange kinetics of oxidized and reduced cytochrome *c* over more than 3 orders of magnitude on the time scale. Cytochrome *c* solutions were placed in D_2O in the reduced and oxidized forms (pH* 7, 20 °C). Samples were taken after 0.33, 1, 3, 9, 27, 92, 213, and 717 h of exchange, reduced, and quenched into slow-exchange conditions (low pH and temperature). Identical acquisition and processing parameters were used for all 16 samples (see Experimental Procedures). Figure 1 shows representative *J*-correlated contour spectra in the "fingerprint" spectral region containing the NH–C_αH cross peaks.

At the initial H-exchange time point, after 20 min of exchange with D_2O in the reduced form, 54 amides still produced clearly visible NH–C_αH cross peaks. Forty of these have previously been assigned in the cytochrome *c* molecule (Wand & Englander, 1985). In the last spectrum of the exchange series, after 1 month of exchange, 22 amide cross peaks in the reduced form and 17 in the oxidized form are still visible above the noise level. Among these, the intensity of eight peaks in the reduced protein and five in the oxidized form did not detectably decrease over the entire exchange period.

The cross peaks assigned to residues 8–15 are labeled in Figure 1, and individual proton-exchange rates, obtained from the decrease in cross-peak intensity with exchange time (Figure 1–4), are listed in Table I. The amide cross peaks of Lys-5,

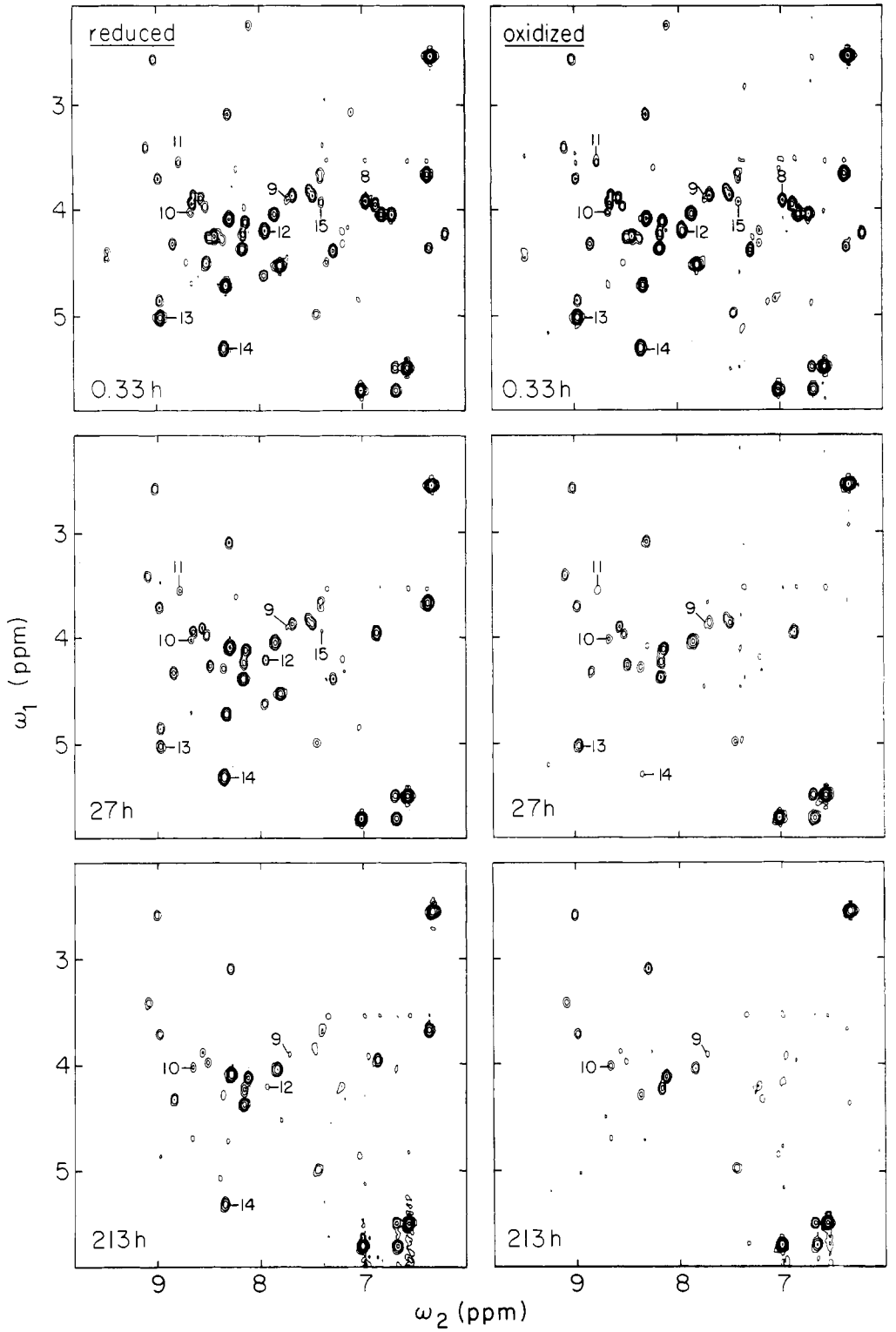

FIGURE 1: Representative *J*-correlated spectra of cytochrome *c* after exchange at pH* 7, 20 °C, in the reduced (left) and oxidized (right) form. The spectral region containing the NH–C_αH cross peaks is shown in the contour presentation. The cross peaks assigned to residues 5–15 (Wand & Englander, 1985) are labeled. Spectra were recorded at 500 MHz in the reduced form at pH* 5 and 20 °C.

Gly-6, and Lys-7 are visible in H_2O solution and disappear during the first 20 min of exchange in D_2O (at pH* 7, 20 °C), so that their exchange rate must be greater than 10 h^{-1}. At the other extreme, the NH of Phe-10 did not exchange over the duration of the experiment, setting an upper limit of 10^{-4} h^{-1} for its rate. The latter estimate can be improved by referring to the early data of Patel & Canuel (1976), who measured exchange rates by one-dimensional NMR at several conditions of pH and temperature for some of the most slowly exchanging cytochrome *c* protons. Among these is the NH resonance assigned to Phe-10 by Wand and Englander (1986) [resonance F in Patel & Canuel (1976)], for which Arrhenius temperature dependence was observed between 45 and 65 °C in the reduced form at pH* 7. Extrapolation to 20 °C yields an exchange rate of about 10^{-5} h^{-1} under our conditions. This estimate represents a lower limit since the activation energy for exchange is probably smaller at temperatures below 45 °C (Richarz et al., 1979; Hilton & Woodward, 1979). Together with the limit set by our data, the rate of the Phe-10 NH therefore can be placed between 10^{-5} and 10^{-4} h^{-1}.

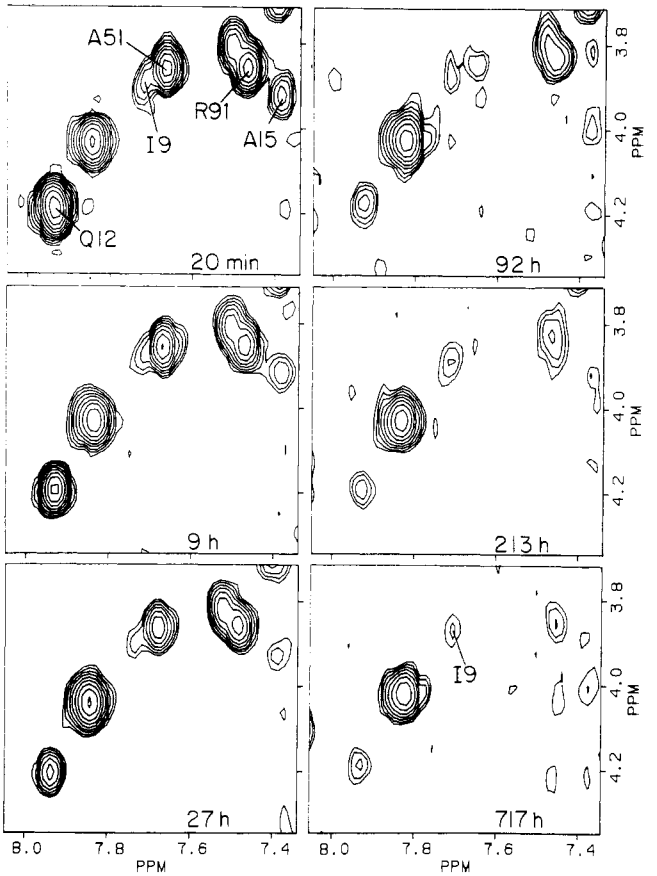

FIGURE 2: Expanded region of the 2D J-correlated spectra recorded in the hydrogen-exchange experiment with reduced cytochrome c. Assigned NH–C_αH cross peaks (Wand, 1984; Wand & Englander, 1986) are indicated.

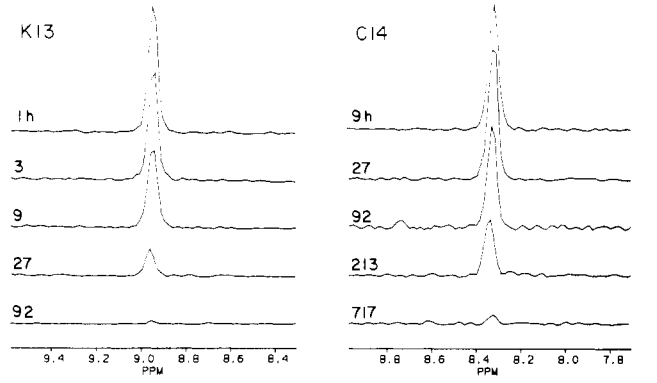

FIGURE 3: Cross sections along ω_2 through the NH–C_αH cross peaks of Lys-13 and Cys-14 at several time points of the exchange experiment with reduced cytochrome c (Figure 1).

The expanded contour plot in Figure 2 and examples of cross sections traced through some COSY cross peaks, shown in Figure 3, illustrate the signal to noise ratio of the data. The statistical error of the exchange rate, on the basis of the variance of the exponential regression, is less than 15% for all except one amide (Table I). A number of factors contribute to the experimental uncertainty. Initial cross-peak intensities differ considerably due to the range of NH–C_αH coupling constants. Quantitation of some cross peaks is hampered by the presence of "t_1 noise" from the slowly relaxing aromatic protons. Residual ^{1}H in the solvent was typically less than 2% but varied somewhat from sample to sample. Variation in the magnetic field homogeneity critically affects the intensity of J-correlated cross peaks due to their antiphase nature and the strong digital filter used. Some cross peaks in crowded

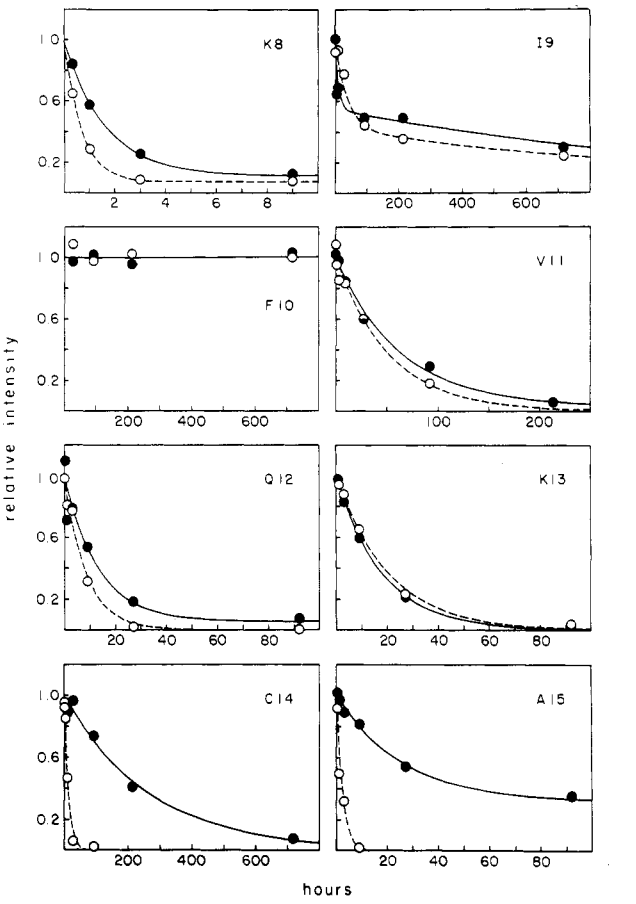

FIGURE 4: Normalized intensity of the NH–C_αH cross peaks of residues 8–15 in reduced (●) and oxidized (○) cytochrome c as a function of exchange time. Solid (reduced) and dashed (oxidized) curves were calculated by exponential least-squares analysis, resulting in the exchange rates given in Table I. First-order exchange kinetics was observed in all cases, except for the Ile-9 cross peak, which shows rapid initial decay due to an overlapped, more rapidly exchanging cross peak (see Figure 2).

regions of the spectrum suffer from partial overlap. Partial exchange of some protons during the 6-h data acquisition period introduces additional line broadening along the ω_1 axis.

Quantitation of the Ile-9 NH exchange rate was particularly difficult. The expanded contour plot in Figure 2 shows the weak NH–C_αH cross peak of Ile-9 partially overlapped with a more intense cross peak assigned to Ala-51 (Wand, 1984), which fortunately is exchanging more rapidly. The rate listed for Ile-9 in Table I is based on the last three time points where its cross peak is well resolved.

In order to extract the structural contribution to exchange at each proton site, we divide the measured exchange rate constant k_{ex} into the intrinsic free peptide rate constant k_c calculated according to Molday et al. [1972; see also Roder et al. (1985b)]. The ratio k_c/k_{ex}, given in Table I, then corresponds to the factor by which a particular proton in the native protein is slowed relative to its expected exchange in a random chain of the same amino acid sequence. The pattern of slowing factors through the N-terminal segment is shown in Figure 5.

Discussion

H Bonding, Local Unfolding, and H Exchange Mechanism. The central role of intramolecular hydrogen bonding in producing slow H exchange and the role of transient H-bond breakage in allowing the H exchange process to proceed have been discussed in detail by Englander and Kallenbach (1984).

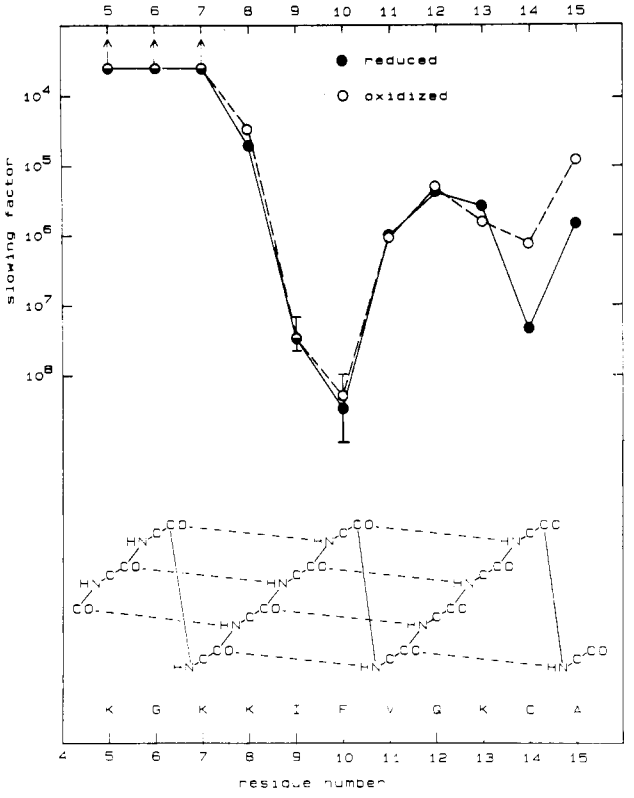

FIGURE 5: Hydrogen exchange behavior in reduced (●) and oxidized (○) cytochrome *c*. The hydrogen-bonding structure in the N-terminal segment is also shown. Relative slowing factors, k_c/k_{ex}, were calculated from the measured rates (k_{ex}, see Table I) with the rules of Molday et al. (1972) to calibrate intrinsic exchange rates, k_c. The schematic drawing of the secondary structure is based on the X-ray model for ferrocytochrome *c* (Takano & Dickerson, 1981).

A large amount of information on model compounds and macromolecules now strongly indicates that the exchange of protein and solvent protons is only possible after preexisting internal H bonds are broken. In this view, the solvent exchange of a protected amide proton can be expressed in terms of the following simple reaction scheme (Hvidt & Nielsen, 1966):

$$\text{Nat(H)} \underset{k_f}{\overset{k_u}{\rightleftharpoons}} \text{Op(H)} \xrightarrow[D_2O]{k_c} \text{Op(D)} \underset{k_f}{\overset{k_u}{\rightleftharpoons}} \text{Nat(D)} \quad (1)$$

Nat represents the native state in which a particular hydrogen is protected from exchange by H bonding, and Op represents all open states that sever the H bond and bring the hydrogen into contact with solvent, permitting the H exchange reaction. Unfolding and refolding rate constants are k_u and k_f, and the chemical exchange rate constant is k_c. Accurate calibrations for predicting k_c from protein sequence (Molday et al., 1972) at any ambient pH and temperature (Englander & Poulsen, 1969; Englander et al., 1978) are available for fully exposed amide NH, and these have been confirmed by exchange measurements of individual protons in an unfolded protein (Roder et al., 1985b).

The present data provide additional evidence for the role of H bonding in retardation of amide proton exchange. There is a close correspondence between the number of slowly exchanging hydrogens and the number of internally H-bonded amide protons. The earliest time spectrum of exchanging ferrocytochrome *c* (Figure 1) exhibits 54 NH–C_αH cross peaks, whereas Takano and Dickerson (1981) identified in the X-ray structure of tuna ferrocytochrome *c* 50 amides H bonded within the protein structure and six more H bonding through internally bound water molecules. It is noteworthy that many of these slowly exchanging peptide NHs are located at the protein–solvent interface. For example, the NH of residues 8 and 12 are on the solvent-exposed surface of the N-terminal helix. Yet, their exchange rates are slowed by a factor of about 10^5 relative to the rate characteristic of non-H-bonded peptides. Some clearly buried amide protons that do not appear in the crystallographic model as H-bond donors (Gly-41 and Thr-49) exchange too rapidly to be measured on the time scale of the present experiments. Though access to solvent is undoubtedly necessary for the H-exchange process, it is evident that relative solvent accessibility in the native state does not determine H exchange rate. The same conclusion has been reached by others [Wagner & Wüthrich (1982a) for BPTI; Kuwajima & Baldwin (1983) for ribonuclease; Englander & Englander (1983) for hemoglobin], who found no correlation between exchange rate of individual amide protons and their placement relative to the native protein surface.

Under most conditions, H exchange from stable proteins appears to occur in the so-called EX2 limit (Hvidt & Nielsen, 1966), in which

$$k_{ex} = (k_u/k_f)k_c = K_{op}k_c \quad (2)$$

where K_{op} is the opening equilibrium constant. Thus, if k_c is known, K_{op} can be directly obtained from the measured exchange rate, k_{ex}, and eq 2. At the other extreme, when exchange is limited by the rate of structural opening, the observed rate is

$$k_{ex} = k_u \quad (3)$$

This opening-limited EX1 case (Hvidt & Nielsen, 1966) has been demonstrated so far only in the pancreatic trypsin inhibitor for a limited range of conditions (Roder et al., 1985a). Although verification of the kinetic limit must await more detailed studies, all previous experience indicates that under the present experimental conditions EX2 behavior is very likely to dominate.

Other work from this laboratory has provided evidence that H-bond breakage reactions important for H exchange do not generally occur as individual, one-bond reactions but involve small segments of structure in cooperative unfolding reactions that may sever several H bonds together (Englander, 1975; Englander & Kallenbach, 1984). In this view, the observed H exchange slowing factor measures K_{op}, the local opening equilibrium constant, and through this measures the free energy difference ΔG_{op}, between the native and opened forms, as in eq 4a. If so, then when changes in H exchange occur,

$$\Delta G_{op} = -RT \ln K_{op} \quad (4a)$$

$$\delta\Delta G_{op} = -RT(\delta \ln K_{op}) \quad (4b)$$

for example, between reduced and oxidized forms of cytochrome *c*, this presents the possibility of resolving localized, functionally important changes in the free energy of structural stability, as suggested in eq 4b. Another important prediction of these relationships is that changes that are more important functionally (energetically) will produce larger, more obvious changes in the H exchange rate. Evidence for this kind of cooperative unfolding behavior is described below.

N-Terminal Helix. The X-ray structure of horse cytochrome *c* (Dickerson et al., 1971) shows that the N-terminal segment forms a helix extending to Ala-15, as diagrammed in Figure 6. The 2.8-Å structure, however, is not accurate enough to define the beginning of the helix. In the closely related tuna ferrocytochrome *c* structure, which could be refined to 1.5 Å (Takano & Dickerson, 1981a), the helix appears to begin at residue 3, so that the first H-bonded NH is that of Lys-7. Table I shows that Lys-8 was the first amide in the

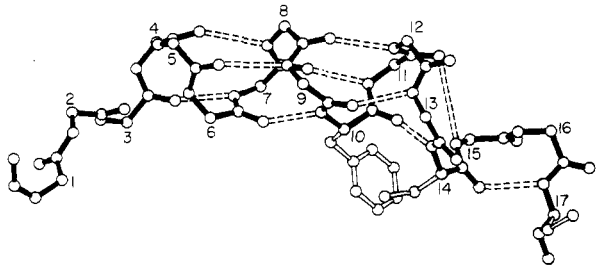

FIGURE 6: Computer representation of the N-terminal segment in the tuna ferrocytochrome *c* structure (Takano & Dickerson, 1981). Nonhydrogen backbone atoms and the side chains of Cys-14 and Cys-17, which bind the heme, and of Phe-10 are shown. C_αs are labeled with residue numbers. Hydrogen bonds are indicated by dashed lines. In this view, the body of the protein lies below the helix and toward the viewer; the H-bond from residue 12 to residue 8 is on the fully aqueous face, and that from residue 14 to residue 10 is fully buried.

N-terminal segment to exchange slowly enough to be measured. However, since faster rates ranging up to the free peptide rate, ca. 10^4 h^{-1}, have not yet been measured in this work, H bonding of Lys-7 cannot be excluded.

Figure 5 displays the hydrogen-exchange rate profile along the N-terminal sequence in terms of the relative slowing factor k_c/k_{ex}. Also shown in Figure 5 is a schematic representation of the H-bonding structure in the region between residue 4 and residue 15 (see also Figure 6). All the amide NHs from residue 8 to residue 15 are involved in H bonds, and all are retarded relative to free peptides by a factor larger than 3×10^4.

Dynamic Fraying at the N-Terminus. From Lys-7 to Phe-10, the exchange rate decreases in a stepwise manner. Each amide exchanges more slowly than the preceding one by 10-fold or more. Between Lys-8 and Ile-9, the protection factor increases by over 1000-fold, and the total decrease over four residues is more than a factor of 10^5 (Table 1; Figure 5). The same pattern occurs in both oxidation states. Similar behavior has been observed in other proteins at the end of α-helices, namely, the S-peptide helix in ribonuclease S (Kuwajima & Baldwin, 1983) and the central helix of bull semin trypsin inhibitor (BUSI IIA) (Wüthrich et al., 1984). In all cases, a significant rate decrease occurs over three to four residues from the N-terminal helix end. The extent of the decrease varies.

This pattern clearly suggests the dynamic fraying behavior expected to occur at the end of a helix [e.g., Zimm & Bragg (1959)]. In the N-terminal helix of cytochrome *c*, opening of the H bond donated by residue 8 can be achieved by rotation about a single dihedral angle at the α-carbon of Lys-5 (to withdraw the acceptor carbonyl of Glu-4). In a fraying mechanism, the probability for opening the second H bond, connecting residue 9 to 5, is smaller since the movement of the residue 5 carbonyl necessary to separate the bond can only occur during the fraction of time when the preceding residue (Glu-4) is free. In terms of eq 4, the opening equilibrium constant for the second bond is reduced since it is determined by the summed free energy required for breaking both bonds simultaneously. Similarly, the probability for breaking the third bond, from residue 10 to residue 6, is still lower.

For model helices, such end effects are formally described by the statistical–mechanical theory of cooperative helix–coil transitions (Zimm & Bragg, 1959; Poland & Scheraga, 1967), which relates the gradient in opening equilibrium constant to the *s* value of the Zimm–Bragg formation. The step values found in the N-terminal cytochrome *c* helix and in the other proteins referred to above are large compared to the *s* values typically obtained for synthetic helical polypeptides [ca. 1, e.g., Scheraga (1978)]. In proteins, interactions of the helix with the rest of the molecule produce additional stabilization.

The differing gradients of fraying behavior observed in the several proteins so far studied presumably reflect interesting details of the helix–protein interactions. The same is true of the wide range of exchange rates in helices of different proteins and in different helices within a given protein. Further study of these issues promises to provide fundamental information on the modes of protein structure formation and stabilization. For now, we emphasize the significance of the fraying behavior observed here and in other similar cases for understanding the protein H exchange mechanism. No such behavior is expected if one takes the view that H exchange can occur without H-bond breakage or that H bonds within a helix can effectively sever independently.

Local Unfolding. The fraying behavior that governs exchange of residues 7–10 appears to halt at Phe-10. A more rapid pathway is able to dominate H exchange of the subsequent amides.

In oxidized cytochrome *c*, the peptide NHs of Val-11, Gln-12, Lys-13, and Cys-14 all experience a similar degree of retardation (Figure 5). They exchange at a rate slower than free peptides by roughly 1 000 000-fold, yet all are within a factor of 3 of their average rate. The Ala-15 NH is somewhat faster than the rest of the group. In native cytochrome *c*, the NH of residues 11, 12, and 15 are on the aqueous surface of the protein, residue 13 is partially exposed, and Cys-14, which forms the covalent heme bridge, is fully buried. Nevertheless, all exhibit very similar rates of exchange with solvent. The common exchange behavior of these five sequential amides (four if Ala-15 is excluded) suggests that they are exposed to exchange with solvent in a single, cooperative structural transition. Apparently, the helix is distorted in such a way that this sequence of H bonds is severed, and all the amide NHs are brought, roughly equally, into H-bonding contact with solvent where exchange can proceed. It may seem that the distortion required to achieve this for a single one of the more exposed residues, e.g., Gln-12 alone, would be minimal. Since all these residues, the normally exposed ones and the fully buried ones, are made equally accessible in the H-exchange state, more substantial chain unfolding reactions that break all four H bonds together must be considered. The data indicate that the breaking of a single H bond such as that of the fully exposed Gln-12, in a way that can allow its exchange with solvent, must have an effective K_{op} less than 10^{-6}.

One possible kind of cooperative unfolding is that a stretch of helix peels away at the N-terminal end of this segment and removes the H-bond CO acceptors (residues 7 to 10 or 11), as in the fraying previously discussed. This possibility can be ruled out since it would also sever the H bonds protecting Phe-10 and prior residues (see Figure 6 and the diagram at the bottom of Figure 5) and thus would produce more rapid exchange for those residues than is observed. The unfolding then must involve the stretch of chain to the right (Figure 5) of the Phe-10 NH. It is possible to sever the H bonds in question simply by "pulling out" the C-terminal end of the helical segment. The opening required must extend from Phe-10 to Cys-14 at least, presumably involving single-bond rotations about these and the intervening α-carbons. The same opening reaction would also sever the H-bond from Ala-15 NH to Val-11 CO. In the oxidized protein, the Ala-15 NH proton exchanges somewhat faster than the other protons in this group. This may represent an independent, more probable (larger K_{op}) unfolding reaction (made possible by the sharp

turn in structure at Cys-14) that frees the Ala-15 NH by moving it away from its acceptor in the helix.

As a possible cause for the abrupt termination of the cooperative unfolding reaction at Phe-10, we note that this residue lies between the N-terminal helix and the bulk of the protein and the phenyl ring is buried (Figure 6). The occurrence of highly retarded amide protons at the interface between helices and the protein core, involving large buried side chains, appears to be a fairly general phenomenon. Such cases were noted in the C-terminal helix of trypsin in a neutron diffraction study by Kossiakoff (1982), where the only unexchanged amide sites on the helix were those of Ile-238 and Ile-242 located in a contact with two strands of β-sheet, in myoglobin which was also studied by neutron diffraction (Schoenborn, 1985), in the central helix of BUSI IIA (Wüthrich et al., 1984) where the amides of Phe-38 and Val-42 are the most highly protected ones, and in the S-peptide helix of ribonuclease S (Kuwajima & Baldwin, 1983) where the highest degree of protection is observed for the backbone NH of the buried His-12 residue.

Although Cys-14 is included in the unfolding unit suggested for the oxidized protein, its slowing factor in the reduced protein is greater, by about 50-fold, than those of its neighbors. A slowing in the Ala-15 rate also occurs, and its rate becomes very close to those of residues 11–13. This behavior might represent a change in stability near the heme in the native state or a change in the average conformation of the unfolded state. The molecular structure in this region (Figure 6) suggests that an opening similar to the one just described for the oxidized state can produce this exchange pattern. Here, it is necessary to pull out the chain segment from residue 11 to the α-carbon of residue 13 (rather than residue 14 or beyond as before). This would sever the H bonds donated by residues 11–13 as well as the Ala-15 NH bond (accepted by the Val-11 CO) and produce similar H-exchange rates for these protons, as the H-exchange data require, but might conserve the Cys-14 to Phe-10 H bond. Alternative possibilities can be considered; e.g., it cannot be ruled out that differences in the average conformation of the reduced form open state act to protect the Cys-14 NH or even that residues 14 and 15 may form a separate unfolding unit.

Results pointing to cooperative unfolding units in five other proteins have been previously reported [pancreatic trypsin inhibitor by Wagner & Wüthrich (1982), ribonuclease S by Kuwajima & Baldwin (1983), apamin by Wemmer & Kallenbach (1983), hemoglobin by Englander & Englander (1983), and BUSI IIA by Wüthrich et al. (1985); reviewed in Englander & Kallenbach (1984)]. In each case, four to eight residues in a helical sequence, some on the external aqueous face and some fully buried, all exchange with similar slowing factors, ranging from 10^2 to 10^6 for the different helices. This is the result expected for a local unfolding mechanism and is very difficult to understand on any other basis.

At a finer level of resolution, one finds among the protons in each unfolding unit deviations of the various exchange rates from exact equivalence. For example, in ferricytochrome *c*, residues 11–14 all exchange at similar rates, but there is some "fine structure" variation among them. The overall variation is 6-fold in cytochrome *c* compared to an average rate 10^6 times slower than the free peptide rate, 10-fold in BPTI compared to an average slowing factor of 10^4 (six residues), 3-fold in BUSI IIA compared to an average slowing factor of 3×10^3 (five residues), 3-fold in ribonuclease S peptide compared to an average slowing factor of 10^3 (five residues), and 3-fold in apamin compared to an average slowing factor of 100 (five residues). According to eq 2, these variations in rate may reflect small variations in effective K_{op} or in k_c (eq 2) due to structural details of the native structure or the unfolded form.

In summary, the results suggest that H exchange of residues 11–14 in oxidized cytochrome *c* is determined by a local conformational unfolding reaction that extends from the Phe-10 α-carbon to at least Cys-14 and exposes also the Ala-15 NH. A similar unfolding reaction appears to occur in the reduced form. Results for the more N-terminal residues convincingly display the fraying behavior expected at the free end of a helix. Similar results, suggesting cooperative unfolding of helical segments and fraying at helix termini, have been found in other proteins.

Effect of Oxidation State. Comparison of H exchange in the reduced and oxidized forms of cytochrome *c* can help to illuminate the effect of a local perturbation, the addition of one unit of positive charge at the heme iron, on local structure and dynamics throughout the protein and thus may indicate the ways in which the protein structure interacts more favorably with the reduced state of the heme to set the redox potential.

In agreement with the crystallographic results of Takano and Dickerson (1981b), we find that the H-bonding structure in the N-terminal region is conserved in the two oxidation states. No hydrogens were found that appear H bonded in one state and free in the other. The sequence from residue 8 through 13, where redox-dependent changes in H-exchange rate are smaller than a factor 2, coincides with one of the least affected regions in the X-ray study. In the N-terminal segment studied here, significant changes occur only very near the heme. The exchange rate of Cys-14, which forms one of the covalent protein–heme bridges, is slowed in the reduced relative to the oxidized state by a factor of 17, and the adjacent Ala-15 NH experiences a 9-fold slowing in the reduced form, bringing it within the range of slowing factors experienced by residues 11–13.

In the rest of the protein, unlike the X-ray results in which only minor changes are seen, the exchange of some protons is greatly affected by the change in redox state. Hydrogen exchange is sensitive not only to the static protein structure but also to structural dynamics and therefore reflects local stability and strain. A fuller appreciation of these effects must await more complete resonance assignments.

Free Energy. Equations 4a and 4b suggest that, insofar as H exchange rates relate to structural unfolding equilibria, H exchange results might be used to measure local structural stability in real free-energy terms and to correlate energetic changes in internal protein interactions with the different protein functional states.

If one assumes that the structural opening detected here behaves like a two-state unfolding transition, then the free energy associated with this opening equilibrium, calculated from the H-exchange rates according to eq 4a, is about 8 kcal/mol. For the more stable Phe-10 NH, the calculated value is between 11 and 12 kcal, within the range of values estimated for complete protein unfolding [from denaturation studies of ferricytochrome *c* by Privalov & Kechinashvilli (1974) and Knapp & Pace (1974)]. It is therefore possible that the NH of Phe-10 is exposed only upon major unfolding of the protein.

Quantitative interpretation in these terms, however, is complicated, as with all equilibrium measurements, by the possibility that exchange rates can be altered either by effects on the stability of the native state, which one wishes to study,

or by effects on the open state. Pending the resolution of these uncertainties, one should take free-energy values calculated from H exchange rates as a qualitative estimate of stability and stability change rather than as a strict quantitative measure.

Registry No. Cytochrome *c*, 9007-43-6.

REFERENCES

Aue, W. P., Bartholdi, E., & Ernst, R. R. (1976) *J. Chem. Phys. 64*, 2229–2246.

Bax, A. (1982) *Two-Dimensional Nuclear Magnetic Resonance in Liquids*, Reidel, London.

Churg, A. K., Weiss, R. M., Warshel, A., & Takano, T. (1983) *J. Phys. Chem. 87*, 1683–1694.

DeVault, D. (1980) *Q. Rev. Biophys. 11*, 387–564.

Dickerson, R. E., & Timkovich, R. (1975) *Enzymes (3rd Ed.) 11*, 397–547.

Dickerson, R. E., Takano, T., Eisenberg, D., Kallai, O. B., Samson, L., Cooper, A., & Margoliash, E. (1971) *J. Biol. Chem. 246*, 1511–1535.

Eden, D., Mathew, J. B., Rosa, J. J., & Richards, F. M. (1982) *Proc. Natl. Acad. Sci. U.S.A. 79*, 815–819.

Englander, S. W. (1975) *Ann. N.Y. Acad. Sci. 244*, 10–17.

Englander, S. W., & Poulsen, A. (1969) *Biopolymers 7*, 379–393.

Englander, S. W., & Englander, J. J. (1983) in *Structure and Dynamics of Nucleic Acids and Proteins* (Clementi, E., & Sarma, R. H., Eds.) pp 421–433, Adenine Press, New York.

Englander, S. W., & Kallenbach, N. R. (1984) *Q. Rev. Biophys. 16*, 521–655.

Englander, J. J., Calhoun, D. B., & Englander, S. W. (1979) *Anal. Biochem. 92*, 517–524.

Ferguson-Miller, S., Brautigan, D. L., & Margoliash, E. (1977) *Porphyrins 7B*, 149–240.

Freeman, R., & Morris, G. A. (1979) *Bull. Magn. Reson. 1*, 5–26.

Hilton, B. D., & Woodward, C. K. (1979) *Biochemistry 18*, 5834–5844.

Hopfield, J. J. (1974) *Proc. Natl. Acad. Sci. U.S.A. 71*, 3640–3644.

Hvidt, A., & Nielsen, S. O. (1966) *Adv. Protein Chem. 21*, 287–386.

Kassner, R. J. (1972) *Proc. Natl. Acad. Sci. U.S.A. 69*, 2263–2267.

Knapp, J. A., & Pace, C. N. (1974) *Biochemistry 13*, 1289–1294.

Kossiakoff, A. A. (1982) *Nature (London) 296*, 713–721.

Kuwajima, K., & Baldwin, R. L. (1983) *J. Mol. Biol. 169*, 299–323.

Marcus, R. A. (1964) *Annu. Rev. Phys. Chem. 15*, 155–196.

Margoliash, E., & Schejter, A. (1966) *Adv. Protein. Chem. 21*, 113–286.

Margoliash, E., & Bosshard, H. R. (1983) *Trends Biochem. Sci. (Pers. Ed.) 8*, 316–320.

Molday, R. S., Englander, S. W., & Kallen, R. G. (1972) *Biochemistry 11*, 150–158.

Moore, G. R. (1983) *FEBS Lett. 161*, 171–175.

Moore, G. R., Huang, Z. X., Eley, C. G. S., Barker, H. A., Williams, G., Robinson, M. N., & Williams, R. J. P. (1982) *Faraday Discuss. Chem. Soc. 74*, 311–329.

Nagayama, K., Kumar, Anil, Wüthrich, K., & Ernst, R. R. (1980) *J. Magn. Reson. 40*, 321–334.

Patel, D. J., & Canuel, L. L. (1976) *Proc. Natl. Acad. Sci. U.S.A. 73*, 1398–1402.

Poland, D., & Scheraga, H. A. (1967) in *Poly-α-Amino Acids* (Fasman, G. D., Ed.) Dekker, New York.

Privalov, P. L., & Khechinashvili, N. N. (1974) *Biofizika 19*, 10–15.

Richarz, R., Sehr, P., Wagner, G., & Wüthrich, K. (1979) *J. Mol. Biol. 130*, 19–30.

Roder, H., Wagner, G., & Wüthrich, K. (1985a) *Biochemistry 24*, 7396–7407.

Roder, H., Wagner, G., & Wüthrich, K. (1985b) *Biochemistry 24*, 7407–7411.

Salemme, F. R. (1977) *Annu. Rev. Biochem. 46*, 299–329.

Scheraga, H. A. (1978) *Pure Appl. Chem. 50*, 315–324.

Schoenborn, B. P. (1985) *Biophys. J. 47*, 34a.

Senn, H., Keller, R. M., & Wüthrich, K. (1980) *Biochem. Biophys. Res. Commun. 92*, 1362–1369.

Stellwagen, E. (1978) *Nature (London) 275*, 73–74.

Takano, T., & Dickerson, R. E. (1981a) *J. Mol. Biol. 153*, 79–94.

Takano, T., & Dickerson, R. E. (1981b) *J. Mol. Biol. 153*, 95–115.

Ulmer, D. D., & Kägi, J. H. R. (1968) *Biochemistry 7*, 2710–2717.

Wagner, G., & Wüthrich, K. (1982a) *J. Mol. Biol. 160*, 343–361.

Wagner, G., & Wüthrich, K. (1982b) *J. Mol. Biol. 155*, 347–366.

Wand, A. J. (1984) Ph.D. Thesis, University of Pennsylvania.

Wand, A. J., & Englander, S. W. (1985) *Biochemistry 24*, 5290–5294.

Wand, A. J., & Englander, S. W. (1986) *Biochemistry* (preceding paper in this issue).

Wemmer, D. E., & Kallenbach, N. R. (1983) *Biochemistry 22*, 1901–1906.

Wider, G., Macura, S., Kumar, Anil, Ernst, R. R., & Wüthrich, K. (1984) *J. Magn. Reson. 56*, 207–234.

Wüthrich, K., Wider, G., Wagner, G., & Braun, W. (1982) *J. Mol. Biol. 155*, 311–319.

Wüthrich, K., Strop, P., Ebina, S., & Williamson, M. P. (1984) *Biochem. Biophys. Res. Commun. 122*, 1174–1178.

Zimm, B. H., & Bragg, J. K. (1959) *J. Chem. Phys. 31*, 526–535.